

Molecular quantum-dot cellular automata: From molecular structure to circuit dynamics

Yuhui Lu, Mo Liu, and Craig Lent^{a)}

Department of Electrical Engineering, University of Notre Dame, Notre Dame, Indiana 46565

(Received 23 February 2007; accepted 25 June 2007; published online 13 August 2007)

We establish a method for exploring the dynamics of molecular quantum-dot cellular automata (QCA) devices by hierarchically combining the techniques of quantum chemistry with the nonequilibrium time-dependent coherence vector formalism. Single QCA molecules are characterized using *ab initio* quantum chemistry methods. We show how to construct a simple model Hamiltonian for each QCA cell based on parameters extracted from the *ab initio* calculation. The model Hamiltonian captures well the relevant switching behavior and can then be used to calculate the time-dependent coherence vector, including thermal and nonequilibrium behavior. This enables us to explore dynamic behavior and power dissipation for various QCA devices and circuits. © 2007 American Institute of Physics. [DOI: 10.1063/1.2767382]

I. INTRODUCTION

Quantum-dot cellular automata (QCA) provides an alternative paradigm¹ for the design of molecular electronics. In the QCA approach, binary information is stored in the charge configuration of single cells and transferred via Coulomb coupling between neighboring cells. Decreased resistive heating makes possible extremely high device densities without dissipating catastrophic amounts of energy.² The operational principles of QCA devices have been extensively studied both theoretically³ and experimentally.^{4,5}

The theory of QCA devices and circuits has seen considerable development over the past decade.^{6–8} Figure 1 schematically shows three charge configurations of a six-dot cell which correspond to logic states. The two polarized charge configurations of $P=1$ and $P=-1$ represent binaries “1” and “0,” respectively. The electrons can be pulled into the null state ($P=0$) by reducing the occupation energy of central dots, which can be implemented by changing the clocking potential applied to the central dots. Cell configurations for binary wire, inverter, and the basic logic elements of the QCA architecture⁷ are shown in Fig. 2. Clocking provides a means for controlling the flow of information through large arrays composed of these fundamental QCA elements. Clocked switching involves pulling the electrons from a polarized state into a null state and pushing the electrons out of the null state and into a new polarized state. Landauer and Keyes⁹ proposed this method of quasiadiabatic switching which has been adapted for use in six-dot cells. Adiabatic clocking maintains the cell arbitrarily close to its ground state throughout the switching process, so the adiabatic theorem guarantees that if the switching is performed gradually enough it can be accomplished with an arbitrarily small amount of energy dissipation, as has been demonstrated in our recent studies.¹⁰

When QCA cells downsize to the molecular scale, each cell becomes a single molecule. The bistable charge configu-

ration of QCA cells can be provided by the localized states of the mix-valence complexes.¹¹ Several candidate QCA molecules have been synthesized and characterized.^{12,13} These candidate molecules have shown switching behavior under an external field, which satisfies the basic requirement of QCA cells. Quantum chemistry *ab initio* techniques have also been employed to study the electronic structure of candidate molecules.^{14,15} These calculations confirm the bistable charge configuration and possibility of information process via the intermolecular Coulomb interaction.

Because QCA devices transfer information through Coulomb interactions, the understanding of molecular interaction is of crucial importance to understand the dynamics of QCA circuits. Although electron transfer (ET) of thermal excitation and optical excitation has been thoroughly explored both experimentally¹⁶ and theoretically,^{17,18} the study of Coulomb interaction-induced ET is rare. Recent studies^{19,20} of self-assembled monolayers (SAMs) of mixed-valence complexes show that when the mole fraction of electroactive groups is high, the effect of intermolecular interaction on the ET rate constant is non-negligible, which suggests that further investigation of molecular interaction-induced ET is necessary for future molecular electronics. Furthermore, from the point view of “bottom-up” design of nanoelectronics, it requires a natural development of a theory to understand the circuit dynamics based on the structure of the individual device “at the bottom.”

The development of quantum chemistry in the past half century provides a rather reliable technique to explore the electronic structure of single molecules.²¹ However, the dynamical study of QCA devices, which may involve a large number of molecules, requires more subtle techniques to simplify the calculation—*ab initio* calculation for many complex molecules is not feasible. The number of the basis functions required increases quickly with the number of molecules. Moreover for an open system in contact with a heat bath such as a QCA device attached to a substrate, a pure state wave function is not enough to describe the physics of the system because the system is usually in a mixed state. A

^{a)}Electronic mail: lent@nd.edu

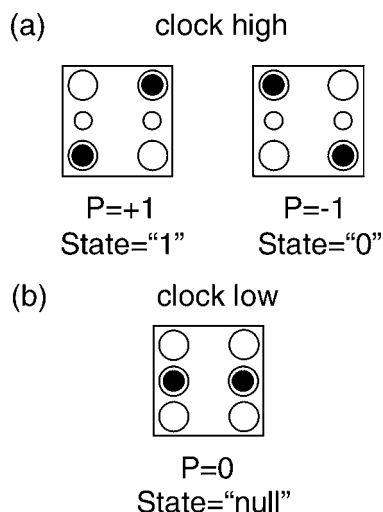


FIG. 1. Schematic of the six site QCA cell. (a) When the occupation energy of the middle dots is high, each electron is essentially localized to a single dot and Coulombic repulsion causes the electrons to occupy antipodal sites within the cell. The two resulting bistable states correspond to cell polarizations of $P=+1$ and $P=-1$. These polarizations have bit values 1 and 0, respectively. (b) When the occupation energy of the middle dots is low enough to overcome the Coulombic repulsion of the electrons, the electrons occupy the middle dots. This configuration is designated the "null" state with $P=0$.

more general density matrix approach is needed to describe the open system.

Our strategy is to conduct a high level *ab initio* calculation on the single molecule and construct a simple model Hamiltonian to describe the molecular switching behavior. We then apply the coherence vector formalism²²⁻²⁴ to solve the dynamic problem. With a model Hamiltonian constructed from state-of-the-art *ab initio* calculation, we calculate the coherence vector of each molecule, from which we can obtain the dynamic behavior of various QCA devices and circuits. In this work, we combine the quantum chemistry *ab initio* technique and coherence vector formalism to investigate two model QCA molecules: 1,5,9-decatriene cation (molecule 1) and 1,10,19-eicosatriene cation (molecule 2). Both molecules have three C=C double bonds, acting as three quantum dots. We compare these two molecules because they have the same redox centers but different structures which lead to different switching behaviors. More complex (and realistic) molecules with metal redox centers await future work.

The remainder of this paper is organized as follows: In Sec. II we present a brief description of the coherence vector formalism. In Sec. III, we calculate the switching behavior of single molecules and construct model Hamiltonians for molecules 1 and 2. The dynamic properties including switching speed and energy dissipation are discussed in Sec. IV. Finally, a summary is given in Sec. V.

II. COHERENCE VECTOR FORMALISM

The details of the coherence vector formalism have been discussed elsewhere.²³⁻²⁵ Here we only present a brief summary description for completeness.

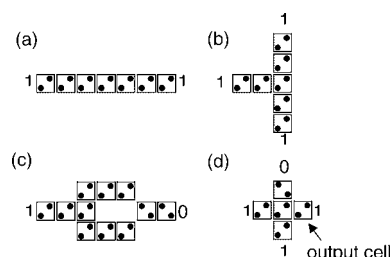


FIG. 2. Fundamental QCA devices. (a) This binary wire transmits data between two points (when clocked it functions as a shift register), (b) fanout provides a method to split a data signal and send the same value to two different destinations, (c) an inverter uses the Coulombic interaction of diagonally aligned cells to invert the input signal, and (d) the majority gate is the fundamental logical element of the QCA architecture where the output is the value corresponding to two or more of the three inputs.

The equation of the motion for the coherence vector, also called the generalized Bloch vector, is given by

$$\frac{d}{dt}\boldsymbol{\lambda} = \boldsymbol{\Omega} \cdot \boldsymbol{\lambda} - \frac{1}{\tau}(\boldsymbol{\lambda} - \boldsymbol{\lambda}_{ss}), \quad (1)$$

where $\boldsymbol{\lambda}$ is the coherence vector of each cell which contains all the real dynamic degrees of freedom of the density matrix. $\boldsymbol{\Omega}$ is given by:

$$\Omega_{ik} = \sum_j f_{ijk} \Gamma_j. \quad (2)$$

Here the f_{ijk} are the structure constants and $\boldsymbol{\Gamma}$ is the vector representation of Hamiltonian. $\boldsymbol{\Gamma}$ is constructed by projecting Hamiltonian matrix \hat{H} onto the generators $\hat{\lambda}_i$ of the group $SU(N)$,

$$\Gamma_i = \frac{\text{Tr}\{\hat{H}\hat{\lambda}_i\}}{\hbar}, \quad (3)$$

N is the dimension of state space for a QCA cell; for the three-dot molecules discussed here, $N=3$ and $\hat{\lambda}$ consists of eight 3×3 matrices. A tabulation of the generators for $SU(3)$ is given in the appendix of Ref. 24.

Energy stored in the molecular configuration can be transported to the substrate through the bonds which anchor the molecule. A detailed description of this would require knowledge of specific molecular vibrational modes as well as substrate modes, and their coupling to the switching electronic states of each molecule. This coupling would depend on the precise construction of the anchoring ligands. The specifics of this process do not concern us here, and the net effect of this energy relaxation pathway is included through the relaxation time τ . Note that energy transported from molecule to molecule is included through intermolecular field-mediated coupling by direct calculation.

$\boldsymbol{\lambda}_{ss}$ in Eq. (1) is the associated time-dependent steady-state coherence vector, which describes the instantaneous thermal equilibrium state. The components of $\boldsymbol{\lambda}_{ss}$ are

$$\lambda_{ss}^{(j)} = \text{Tr}\{\hat{\rho}_{ss}(t)\hat{\lambda}_j\}, \quad (4)$$

where j is an index through the vector components and their corresponding generators. $\hat{\rho}_{ss}(t)$ is the instantaneous thermal

equilibrium density matrix for a time-dependent Hamiltonian,

$$\hat{\rho}_{ss}(t) = \frac{e^{-H(t)/k_B T}}{\text{Tr}\{e^{-H(t)/k_B T}\}}, \quad (5)$$

from the above discussion we can see in the equation of motion (1), both Ω and λ_{ss} are uniquely determined by the Hamiltonian matrix \hat{H} . For the *ab initio* calculation, \hat{H} is calculated by choosing a set of basis functions, for example, Gaussian functions. Typically a basis set of many hundreds of states is required.¹⁵ This is why the high level *ab initio* calculation for an entire multicell QCA circuit is extremely time consuming, if not totally impossible. However, for a three-state molecule used as a QCA cell, we are only interested in the three stable charge configurations representing “0,” “1,” and “null” states, as discussed in Sec. I. Our strategy is to conduct the state-of-the-art *ab initio* calculation on the single QCA cells to determine the three energies corresponding to the 0, 1, and null states, and construct a 3×3 model Hamiltonian with the three-state approximation,^{24,26}

$$H = \begin{bmatrix} E_0 - \varepsilon ed/2 & -\gamma & 0 \\ -\gamma & E_0 + E_c & -\gamma \\ 0 & -\gamma & E_0 + \varepsilon ed/2 \end{bmatrix}, \quad (6)$$

where E_0 is the on-site energy of each state, E_c is the energy provided by the clock, which changes the potential of central dot, thus controls the mobile electrons in and out of the central dots. ε is the switching field (from the neighboring molecules) and d and γ are the effective distance and tunneling energy between the central and edge dots. The *ab initio* calculations on molecules 1 and 2 are used to extract parameters d and γ of the model Hamiltonian, which we can then use to solve the equation of motion (1) to compute the dynamic properties of the cell-cell interactions.

It is worth noting that the model Hamiltonian has two zeroes. They correspond to the spatial separation between the two edge dots. Since the only tunneling channel of the clocked QCA molecule is through a central dot, there is no direct interaction between two active states (see Sec. III), thus the two off-diagonal zeros which appear in the model Hamiltonian are not surprising. The more detailed discussion of the model Hamiltonian of a donor-bridge-acceptor complex can be found in Ref. 26.

III. AB INITIO CALCULATION OF ELECTRONIC STRUCTURE OF SINGLE-MOLECULE CELLS

First, we optimized the geometry of molecule 1, as shown in Fig. 3(a). Three stable charge configurations are obtained by an *ab initio* calculation at Hartree-Fock level²⁷ and a 6-31G basis set. All *ab initio* calculations of this work have been done with GAUSSIAN 03.²⁸ The three stable configurations of 1, corresponding to the charge localization on the different redox sites as shown by the electrostatic potential shown in Fig. 3(b), can be used to represent binary information 0, 1, and null states. The switching of the molecule can be realized by applying two electric fields. A vertical clocking field determines whether the molecule is in the active states or null state, while a horizontal field (from a

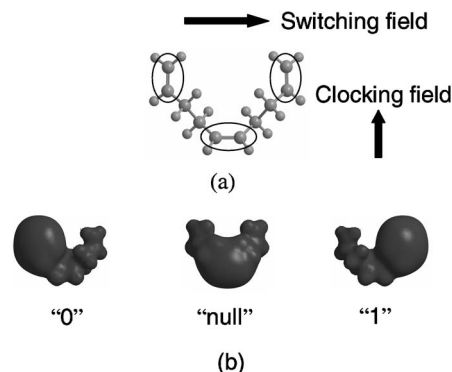


FIG. 3. Molecular structure and three stable charge configurations of model molecule 1. Three ethylene groups function as three quantum dots (a). The electrostatic isopotential surface for the three states obtained from *ab initio* calculations is shown in (b). The mobile charge can localize in three different sites thus represent binary information “0,” “1,” and a “null” state.

neighboring molecule) switches the molecule between 0 and 1 active states.

The switching field and clocking field magnitudes in our calculations approximate those physically reasonable in such a system. For simplicity we are here using a uniform switching field to mimic the effect of a neighboring molecule. Below (see Figs. 7 and 9), the actual nonuniform fields produced by one molecule will be used in calculating the response on a neighboring molecule. The clocking field would typically be applied using buried conductors with sinusoidal clocking voltages applied to sweep the active region across the surface.²⁹ Switching the state of QCA molecules using a buried conductor for a layer of two-dot cells has been demonstrated experimentally using mixed-valence compounds.^{12,30} In those experiments clocking fields as large as a few V/nm were applied.

With the optimized geometry, we calculate the three lowest-lying energy levels as a function of clocking field and a switching field at a complete active space multiconfiguration self-consistent field (CASSCF) level.^{31,32} The calculated energy levels are shown in Fig. 4, from which we can see the interaction between the ground state and low lying excited states, which enables the switching of the mobile charge from one site to another.

When the clocking field is zero, the null state is always the ground state shown in Fig. 4(a). Note that in Fig. 4(a), the lowest energy level corresponds to the null state according to the electronic structure analysis. The first excited state corresponds to 1 state under a negative switching field and 0 state under a positive field. By contrast, the second excited state corresponds to 0 state under a negative switching field and 1 state under a positive switching field. This is easy to understand since under a uniform field, the potential of the central dot remains zero so the energy of null state does not change with the switching field, but the potential of the edge dots changes linearly with the switching field so the energy of 0 and 1 states varies linearly with the switching field. Although two active states show adiabatic coupling, which is demonstrated by the anticrossing behavior of two excited states, they do not interact with the ground state. This explains why the switching field cannot switch the molecule when the clocking field is zero.

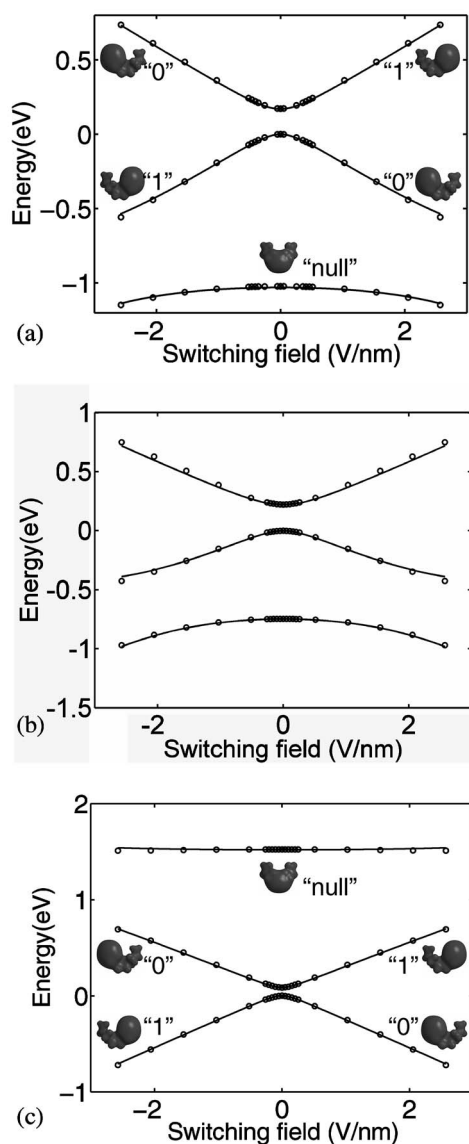


FIG. 4. Three lowest energy levels of molecule 1 under a switching field and various clocking fields: (a) 0 V/nm, (b) 1.5 V/nm, and (c) 10 V/nm. The switching behavior obtained from the fitted model Hamiltonian (solid line) is in good agreement with the *ab initio* calculation at CASSCF(5,6) level (dots). The energy of 0 and 1 states varies linearly with the switching field, while the energy of null state remains unchanged with the switching field.

When a clocking field is turned on as shown in Fig. 4(b), the ground state starts to interact with the excited states. From Fig. 4(b) we can see the clocking field increases the energy of the null state and thus lowers the gap between the null state and active states. The interactions among the lowest energy levels provides strong coupling between the null state and active states. Now the switching field from a nearby molecule could switch the molecule to the appropriate active state.

Finally, when the clocking field is strong enough, the energy of the null state will be much higher than active states, as shown in Fig. 4(c). Although the ground state can be the 0 or 1 state depending on the direction of the switching field, the coupling between two active states is extremely small, as shown by the direct crossing of these two states. This suggests that the mobile charge is locked at a given

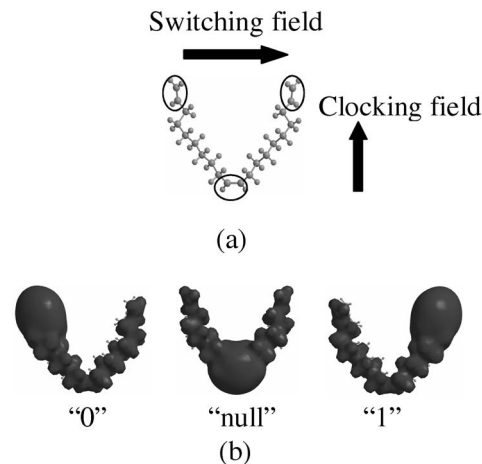


FIG. 5. Molecular structure and three stable charge configurations of model molecule 2. Three ethylene groups function as three quantum dots (a). The electrostatic isopotential surface for the three states obtained from *ab initio* calculations is shown in (b). The mobile charge can localize in three different sites thus represent binary information 0, 1, and a null state.

active state and cannot switch to the other because the energy barrier is too high, which provides the possibility for QCA to be used as memory.^{7,8}

Figure 4 also shows the switching behavior generated from the model Hamiltonian (solid line). Compared with the time-consuming *ab initio* calculation (dot line), diagonalizing the 3×3 model Hamiltonian is much more efficient, while the results are in good agreement with the sophisticated quantum chemistry calculation, which suggests that the 3×3 model Hamiltonian is a good approximation to describe the QCA cell. The fitted values of matrix elements of molecule 1 are given by $\gamma=0.15$ eV and $d=0.18$ nm.

Molecule 1 gives a good example of clocking the cell through a null dot. But from Fig. 4 one can see that the clocking field required to lock may be rather high (10 V/nm in this case), which may be difficult to realize. This problem can be solved by engineering the effective distance between the null dot and the active dots, since the clocking energy $E_c = \varepsilon \ell$, where ε is the clocking field and ℓ is the effective distance between the central dot and edge dots. For a molecule with larger ℓ , a smaller clocking field should be able to control the switching. Molecule 2 (see Fig. 5) has the same redox centers as molecule 1 but has a longer effective distance between the central dot and edge dots, so it is chosen as the other model in this study. The longer arms in molecule 2 mean that a smaller clocking field is required to produce the same energy difference between the active dots and the null dot.

Figure 6 gives the switching behavior of molecule 2 under a switching field and various clocking fields. We can see since molecule 2 has a longer effective distance between the central dot and edge dots, the clocking field required to turn on the device is only about 0.5 V/nm, as shown in Fig. 6(b), and the “holding field” is about 2 V/nm, as shown in Fig. 6(c), which is realizable. The clocking field in the experimental demonstrations of candidate QCA molecules²⁷ has been in the range of a few V/nm. Again, the switching behavior calculated from model Hamiltonian (solid line) is

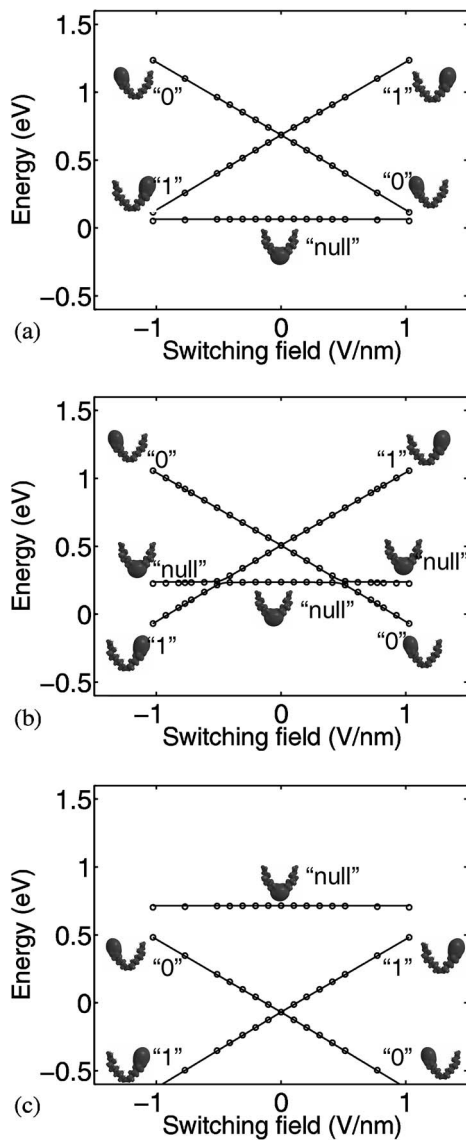


FIG. 6. Energy levels of 2 under a switching field and various clocking fields: (a) 0 V/nm, (b) 0.5 V/nm, and (c) 2 V/nm. The switching behavior obtained from the fitted model Hamiltonian (solid line) is in good agreement with the *ab initio* calculation at CASSCF(5,6) level (dots). The energy of 0 and 1 states varies linearly with the switching field, while the energy of null state remains unchanged with the switching field.

consistent with *ab initio* calculation (dot line). The fitted values of matrix elements of molecule 1 are given by $\gamma = 0.01$ eV and $d = 0.54$ nm.

The *ab initio* calculation also demonstrates that one molecule can switch its neighboring molecule when the clocking field is turned “on.” Figure 7 presents the calculated molecular polarization, given by the molecular dipole moment of 2, along the direction pointing from one edge dot to the other, as a function of the clocking field, while the driver molecule’s polarization is fixed at +1 or –1. In this calculation, a driver molecule is placed next to a target molecule, as shown in the insert of Fig. 7, where the distance of two molecules is set as 11 Å, equal to the distance of two edge dots of molecule 2, thus the four edge dots of two neighboring molecule form a square, mimicking two QCA half cells.³³ With the driver set as fully polarized with the polarization +1 or –1,

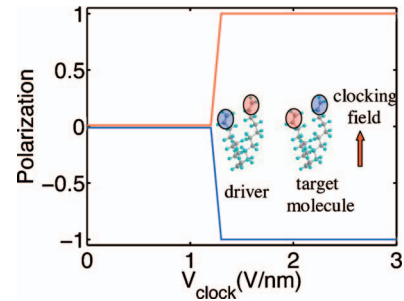


FIG. 7. (Color) The polarization of 2 as a function of the clocking field, while the driver’s polarizations are fixed at +1 (blue curve) and –1 (red curve), respectively. Because of the Coulomb repulsion, two neighboring molecules have the opposite polarization.

we calculate the target molecule’s charge configuration induced by the driver. When the clocking field is zero, the target molecule’s polarization remains zero even though its neighboring molecule is fully activated and polarized. The result of Fig. 7 can be explained by Fig. 6. When the clocking field is low, the ground state corresponding to null state, thus the Coulomb interaction exerted by a neighboring molecule cannot induce an activated state. However, when the clocking field is turned on, the “active” states and null state start to interact with each other, as shown by Fig. 6. Figure 7 shows that the target molecule can be switched to the opposite state by the driver molecule as the target molecule’s polarization reaches +1 or –1 when the clocking field is raised up. (The clocking field “activates” the molecule by driving the mobile charge out of the central dot and the driver molecule switches or “polarizes” the target molecule to its opposite state.)

IV. FROM STRUCTURE TO DYNAMICS

Once the model Hamiltonian is obtained for each QCA cell, we project it onto the generators of SU(3) and convert the Hamiltonian matrix into Hamiltonian vector.²² We then solve the equation of motion (1) in the coherence vector formalism, and through the coherence vector we will obtain all the dynamic information of the QCA circuits. The details of the method can be found in Refs. 24 and 25. We stress that this technique handles both nonequilibrium and thermal effects. In this work, the relaxation time τ of Eq. (1) is fixed at 0.35 ns for all simulations.

We calculate the dynamics of a simple circuit—a QCA shift register including five cells, as shown in Fig. 8. In the calculation, each QCA cell is composed of two model molecules 1, and the distance between two neighboring molecules is fixed at the same value as the two edge dot distance within each molecule, such that every four neighboring edge dots form a square. The model Hamiltonian of molecule 1

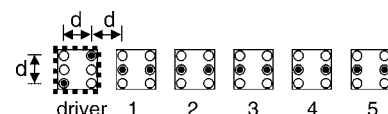


FIG. 8. A QCA shift register composed of five cells numbered from 1 to 5. The distance between neighboring cells equals to the distance between two edge dots of the molecule. $d = 6.8$ Å for molecule 1.

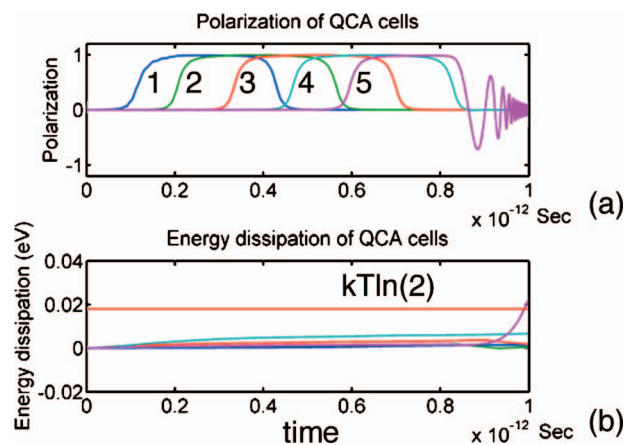


FIG. 9. (Color) Switching dynamics of a QCA wire shown in Fig. 8 with the clock frequencies at 1 THz. The molecular tunneling energy $\gamma=0.15$ eV. (a) The polarization of each cell as a function of time. The blue, green, red, cyan, and magenta curves correspond to the polarization of cells 1–5. Each cell can be polarized by the neighboring molecule through Coulomb interactions when the clocking signal raise up the energy of null state, as shown in Fig. 4. The clocking signal is provided by a sine wave field which propagates from the left to the right. (b) The energy dissipation of each cell during the switching. All cells have a dissipation lower than $kT \ln(2)$ except the last one.

obtained from *ab initio* calculation is applied for all five molecules. For each cell, the electrostatic interactions with all other cells (both the nearest neighbors and the farther neighbors) are included. The coherence vectors of all cells are computed and from which each cell's polarization and energy dissipation are calculated.

In our simulation, the clocking signal is provided by a sine wave field propagating from the left to the right as a function of time. An input signal is set by a driver cell, as shown in Fig. 8. As the clocking signal reaches each cell and turns it on, the Coulomb repulsion of its neighboring cell or driver will switch the cell to the same state, thus the whole system relaxes to its ground state. The more detailed discussion of the clocking organization can be found in Ref. 34.

Figure 9 presents the polarization (the upper panel) and energy dissipation (the lower panel) of each cell as a function of time with the clocking frequency at 1 THz. The five curves given in the upper panels represent the polarization of each cell. As time goes by, the clocking signal reaches five cells one by one, and the cells are switched to the same state as the driver. Figure 9 records the switching behavior of each cell in one clock period. Each cell starts with the zero polarization (corresponding to the null state) and is polarized to 1 state as the clocking signal drives the mobile charge out of the central dots and into the corresponding edge dots as determined by the input signal. On the second half of the period, the clocking signal lowers and the mobile charge tunnels back to the central dot so the polarization becomes zero again.

Because we are calculating the evolution of the cell state while it is in contact with the thermal environment, we can assess energy dissipation in the shift register. Reference 24 does this analysis in greater depth but without the connection to specific molecular properties; γ in Ref. 24 is treated as a parameter—here we calculate it from first principles. Each

cell in the chain moves through a complete cycle from the null state to an active state, then back to the null state. In this full cycle energy flows into the cell from the left neighbor (acting as a driver), out to the right neighbor, from the clock, and to and from the thermal environment. The net energy transfer to the environment, accounted for by Eqs. (1), (4), and (5), is the energy dissipated as heat. The lower panel shows the energy dissipation of each cell as a function of time. For the first four cells, the energy dissipated is lower than $k_B T \ln(2)$, which is in consistent with Landauer's principle³⁵ and the analysis of Ref. 24—there is no fundamental lower limit for energy dissipation if the bit is copied from one cell to another. Only the last cell dissipates an energy more than $k_B T \ln(2)$, which is understandable because as the clocking signals lower at the end of the period, the last cell experiences a nonreversible switching because a bit is erased. We leave further application of this sort of calculation to fundamental questions of dissipation in logically reversible and irreversible molecular circuits to future work.

V. CONCLUSION

In this paper, we describe a well-defined hierarchical theory that connects the detailed molecular quantum chemistry to circuit-level behavior. The electronic structure of single QCA cells and the coupling among the different bit value states are explored by the quantum chemistry *ab initio* technique. The switching physics of QCA cells can be understood from the energy diagrams of the lowest-lying energy levels involved in the switch. A simple 3×3 model Hamiltonian matrix constructed from first-principles calculation captures very well the switching behavior. With the model Hamiltonian, the circuit dynamics are computed by solving the equation of motion using the coherence vector formalism. This method includes the quantum nature of the tunneling and the coupling between the cell and the thermal environment. It is a nonequilibrium, time-dependent, finite-temperature theory. The model Hamiltonian provides a bridge to understand the relations between the cell structure and the circuit dynamics, which enables the design of molecular properties to achieve circuit performance.

¹C. S. Lent, P. D. Tougaw, W. Porod, and G. H. Bernstein, *Nanotechnology* **4**, 49 (1993).

²C. S. Lent, *Science* **288**, 1597 (2000).

³P. D. Tougaw and C. S. Lent, *J. Appl. Phys.* **80**, 4722 (1996).

⁴A. O. Orlov, I. Amlani, G. H. Bernstein, C. S. Lent, and G. L. Snider, *Science* **277**, 928 (1997).

⁵I. Amlani, A. O. Orlov, G. Toth, G. H. Bernstein, C. S. Lent, and G. L. Snider, *Science* **284**, 289 (1999).

⁶C. S. Lent and P. D. Tougaw, *J. Appl. Phys.* **74**, 6227 (1993).

⁷P. D. Tougaw and C. S. Lent, *J. Appl. Phys.* **75**, 1818 (1994).

⁸C. S. Lent and P. D. Tougaw, *Proc. IEEE* **85**, 541 (1997).

⁹R. Landauer and R. W. Keyes, *IBM J. Res. Dev.* **14**, 152 (1970).

¹⁰C. S. Lent, M. Liu, and Y. Lu, *Nanotechnology* **17**, 4240 (2006).

¹¹K. D. Demadis, C. M. Hartshorn, and T. J. Meyer, *Chem. Rev. (Washington, D.C.)* **101**, 2655 (2001).

¹²H. Qi, S. Sharma, Z. Li, G. L. Snider, A. O. Orlov, C. S. Lent, and T. P. Fehlner, *J. Am. Chem. Soc.* **125**, 15250 (2003).

¹³J. Jiao, G. J. Long, F. Grandjean, A. M. Beatty, and T. P. Fehlner, *J. Am. Chem. Soc.* **125**, 7522 (2003).

¹⁴C. S. Lent, B. Isaksen, and M. Lieberman, *J. Am. Chem. Soc.* **125**, 1056 (2003).

¹⁵Y. Lu and C. S. Lent, *J. Comput. Electron.* **4**, 115 (2005).

- ¹⁶A.-C. Ribou, J.-P. Launay, M. L. Sachtleben, H. Li, and C. W. Spangler, *Inorg. Chem.* **35**, 3735 (1996).
- ¹⁷M. D. Newton, *Chem. Rev. (Washington, D.C.)* **91**, 767 (1991).
- ¹⁸M. D. Newton, *Coord. Chem. Rev.* **238–239**, 167 (2003).
- ¹⁹T.-Y. Dong, H.-W. Shih, and L.-S. Chang, *Langmuir* **20**, 9340 (2004).
- ²⁰T.-Y. Dong, L.-S. Chang, I.-M. Tseng, and S.-J. Huang, *Langmuir* **20**, 4471 (2004).
- ²¹W. Kohn, *Rev. Mod. Phys.* **71**, 1253 (1999).
- ²²G. Mahler and V. A. Weberruß, *Quantum Networks: Dynamics of Open Nanostructures* (Springer-Verlag, Berlin, 1998).
- ²³J. Timler and C. S. Lent, *J. Appl. Phys.* **91**, 823 (2002).
- ²⁴J. Timler and C. S. Lent, *J. Appl. Phys.* **94**, 1050 (2003).
- ²⁵J. Timler, Ph.D thesis, University of Notre Dame, 2003.
- ²⁶A. Milischuk and D. V. Matyushov, *J. Chem. Phys.* **118**, 5596 (2003).
- ²⁷C. C. J. Roothaan, *Rev. Mod. Phys.* **23**, 69 (1951).
- ²⁸M. J. Frisch *et al.*, *GAUSSIAN 03*, Gaussian, Inc., Pittsburgh, PA, 1998.
- ²⁹K. Hennessy and C. S. Lent, *J. Vac. Sci. Technol. B* **19**, 1752 (2001).
- ³⁰H. Qi, A. Gupta, B. C. Noll, G. L. Snider, Y. Lu, C. S. Lent, and T. P. Fehlner, *J. Am. Chem. Soc.* **127**, 15218 (2005).
- ³¹M. J. Frisch, I. N. Ragazos, M. A. Robb, and H. B. Schlegel, *Chem. Phys. Lett.* **189**, 524 (1992).
- ³²N. Yamamoto, T. Vreven, M. A. Robb, M. J. Frisch, and H. B. Schlegel, *Chem. Phys. Lett.* **250**, 373 (1996).
- ³³A. O. Orlov, I. Amlani, R. Kummamuru, R. Ramasubramaniam, G. Toth, C. S. Lent, G. H. Bernstein, and G. L. Snider, *Appl. Phys. Lett.* **77**, 295 (2002).
- ³⁴C. S. Lent and B. Isaksen, *IEEE Trans. Electron Devices* **50**, 1890 (2003).
- ³⁵C. H. Bennett, *Int. J. Theor. Phys.* **21**, 905 (1982); see compilation of relevant literature in H. Leff and A. Rex, *Maxwell's Demon 2* (IOP, Bristol, 2003).